

Cite this: *Soft Matter*, 2012, **8**, 3419

www.rsc.org/softmatter

PAPER

Nanostructured poly(ethylene oxide)-like dendron-*block*-linear poly(ethylene-*alt*-propylene) copolymers: design, synthesis, and thermal and assembling properties

Jie Song and Byoung-Ki Cho*

Received 24th November 2011, Accepted 9th January 2012

DOI: 10.1039/c2sm07240h

A series of self-assembling dendron-coil block copolymers with well-defined molecular structures were prepared *via* a divergent method. The hydrophilic and hydrophobic blocks are composed of PEO-like dendrons and poly(ethylene-*alt*-propylene) (PEP) linear coils, respectively. A dendron-coil, **2G-2400** (**2G** and **2400** indicate the dendron generation and PEP molecular weight, respectively), showed a melting transition of the peripheral PEO chains. In contrast, the dendron-coils containing the 3rd generation dendron did not show any melting transition because of the plasticization effect of the tri(ethylene oxide) branches. Due to the strong immiscibility between the PEO-like dendron and PEP blocks, diverse microphase-separated morphologies were observed. **2G-2400** displayed a lamellar mesophase with an interdigitated dendron packing structure. For the larger 3rd generation dendron series, A15 micellar cubic (*Pm3n* space group), hexagonal columnar, and lamellar morphologies were revealed depending on the PEP coil length and/or temperature. For the columnar mesophases, the molecular wedge angles (α) were calculated to be 46.8° and 34.6° for **3G-2400** and **3G-3400**, respectively. This suggests that the longer PEP coil of **3G-3400** is conformationally more deformed in the columnar structure. As a consequence, the columnar phase was transformed into an interdigitated lamellar structure as the temperature increased. This order to order transition is a reversal of the well-known phase sequence of linear block copolymers. This unusual morphological behavior is mainly attributed to the unique molecular arrangement associated with non-conventional dendron-coil chain architecture.

Introduction

The variation of polymer chain topology into non-conventional types has a great influence on the phase behavior in a block copolymer system. Among the possible block copolymer architectures, a dendron-coil architecture is particularly interesting because the two molecular extremes are covalently combined.¹ These blocks are known to have distinct thermal properties such as melting and glass transition temperatures.² In comparison to linear polymers, the branched counterparts have lower melting and glass transition temperatures, and they become completely amorphous in some cases.

Amphiphilic block copolymers, consisting of polyalkylene and poly(ethylene oxide) (PEO) blocks, have a strong segregation tendency in both bulk and solution states. Due to the great immiscibility between the blocks, they are able to form ordered molten structures (mesophases) in a relatively small molecular weight regime. For example, poly(ethyl ethylene)-*b*-poly(ethylene oxide) (PEE-*b*-PEO) copolymers, with molecular weights of

<10 kg mol⁻¹, displayed a variety of mesophases such as lamellar, perforated lamellar, bicontinuous cubic, and hexagonal columnar structures.³ Despite such rich phase behavior, only a crystalline lamellar morphology was observed at room temperature (RT), due to the crystallization of the linear PEO coil. This PEO crystallization occurring above a room temperature is a critical drawback for practical purposes, because a certain material function can be maximized depending on the morphological feature. Therefore, in order to utilize as many structures as possible at room temperature for material applications, an amorphous block has to be used instead of a crystalline one.

In this context, a modification of the linear crystalline PEO into a branched PEO could be an approach for solving the crystallization problem. As a way, we could design PEO-like dendrons based upon tri(ethylene oxide) (TEO) spacers, phloroglucinol branching junctures, and peripheral PEOs. Then, a combination of this type of PEO-like dendron and an appropriate polyalkylene will provide fully amorphous amphiphilic block copolymers. To this end, we prepared a novel series of dendron-coil block copolymers (Fig. 1 and Scheme 2). As a hydrophobic block, we employed linear poly(ethylene-*alt*-propylene)s (PEPs) because this is amorphous and easy to prepare *via* a hydrogenation of polyisoprene (PI). To date, only

Department of Chemistry and Institute of Nanosensor and Biotechnology, Dankook University, Gyeonggi-Do, 448-701, Korea. E-mail: chobk@dankook.ac.kr; Fax: +82 31 8005 3148; Tel: +82 31 8005 3153

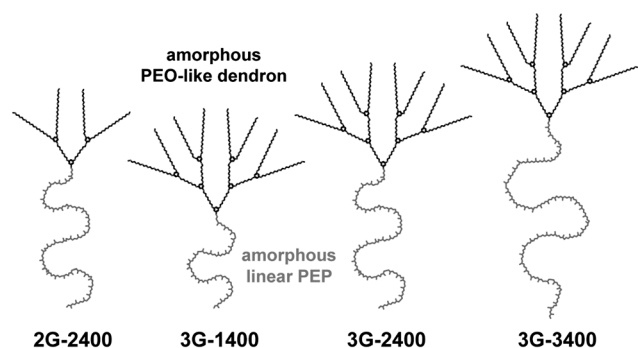


Fig. 1 Schematics of dendron-coils consisting of amorphous PEO-like dendrons and linear PEPs.

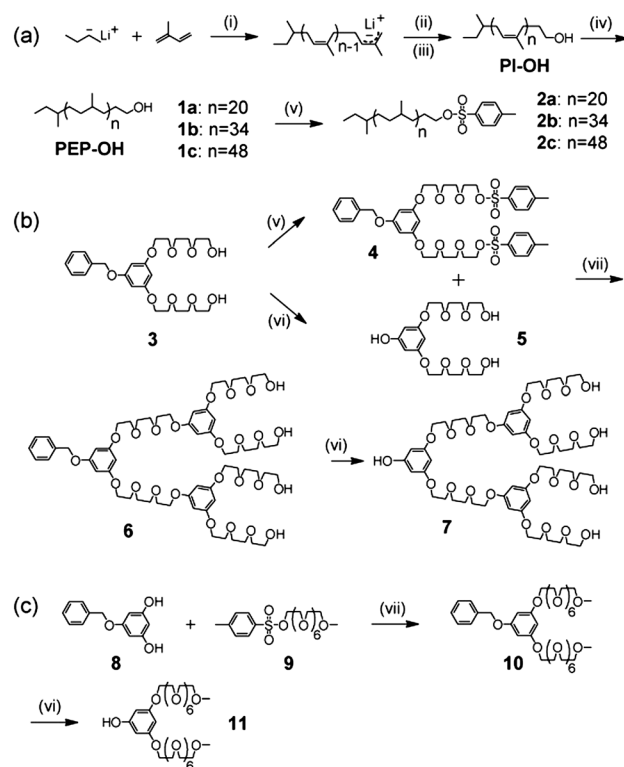
a few block copolymers were reported to contain PEO-like dendron blocks, perhaps because of the difficulty of synthesis.⁴ In most block copolymers, linear PEOs were used as the hydrophilic block.⁵ Therefore, our dendron-coils are topologically unique block copolymers, and this structural feature has a significant influence on the thermal and assembling properties. In this paper, we present the details of the divergent synthesis, and the thermal and self-assembling properties of a series of dendron-coils. To manipulate the mesomorphic behavior, we varied the dendron size and PEP coil length as molecular parameters. One interesting finding was that we observed an unusual phase change (*i.e.*, a columnar-to-lamellar transition) upon heating, and this mechanism was addressed.

Results and discussion

Synthesis

Dendron-coils consist of three structural components: linear PEP, TEO dendritic spacers, and PEO peripheries. In the synthesis, the growth of the branched chain was done mostly with Williamson etherification, debenzoylation, and tosylation. These elemental reactions are known to be conventional and free of side reactions, and their resulting yields were revealed to be very quantitative, generally more than 70%.

Before the divergent dendritic growth, each part was individually prepared, as outlined in Scheme 1. First, linear PEP blocks (**2a–c**) with a tosyl end were prepared by a combination of living anionic polymerization of isoprene, catalytic hydrogenation, and the subsequent tosylation of the hydroxyl end group (Scheme 1(a)). Isoprene was polymerized in cyclohexane using *sec*-butyllithium as the initiator. The polyisoprene (PI) end was then capped with one ethylene oxide unit, and protonated with degassed methanolic HCl, yielding hydroxylated polyisoprenes (**PI-OH**).^{5b} The resulting **PI-OH**s contained 1,4-regioisomeric repeating units (*ca.* 91%), as characterized by the ¹H NMR technique. The **PI-OH**s were then hydrogenated in cyclohexane using Pd/C and H₂. Complete saturation was reached after 48 hours in all cases, as confirmed by no olefin signal at 5.35–4.62 ppm in the ¹H NMR spectra. The number average molecular weights (*M_n*) and the polydispersities (*M_w/M_n*) of the resulting **PEP-OH**s are presented in Table 1. The polydispersities, in all cases, were less than 1.08, which is indicative of their narrow molecular weight distributions. For the next coupling step with



Scheme 1 Synthesis of (a) linear PEP coils (**2a–c**), (b) AB₂- and AB₄-type branching units (**5** and **7**), and (c) diPEGylated phloroglucinol (**11**). *Reagents and conditions:* (i) C₆H₁₂; (ii) ethylene oxide; (iii) methanolic HCl; (iv) 10% Pd/C, H₂, 30 psi, C₆H₁₂; (v) TsCl, pyridine, CH₂Cl₂; (vi) 10% Pd/C, H₂, 30 psi, MeOH/CHCl₃; and (vii) K₂CO₃, KI, CH₃CN.

branching precursors, the hydroxyl end of the **PEP-OH** was converted into a tosyl group.

Hydrophilic branching (**5** and **7**) and peripheral (**11**) precursors were prepared, as shown in Schemes 1(b) and (c). The reason for the preparation of the tetrabranching branching component (**7**) is to simplify the reaction procedure for the 3rd generation dendron-coils. Although a stepwise protocol, starting from dibranched compound **5**, could also be applied in the higher 3rd generation series, tosylation and etherification have to be implemented in each 3rd generation divergent synthesis, which would be tedious in terms of the synthetic scheme.

Dibranching (AB₂-type) and tetrabranching (AB₄-type) components **5** and **7** possess one phenol (A) at the focal point, as well as two and four peripheral aliphatic alcohol groups (B),

Table 1 Characterization of **PI-OH**s and **PEP-OH**s (**1a–c**)

Sample	<i>M_n</i> ^a /g mol ⁻¹	<i>M_w/M_n</i> ^b	DP ^a
PI precursor of 1a	1390	1.11	20
1a	1430	1.08	20
PI precursor of 1b	2340	1.05	34
1b	2410	1.05	34
PI precursor of 1c	3280	1.03	48
1c	3380	1.03	48

^a Determined from the end-group analysis of ¹H-NMR spectra.

^b Determined by the GPC data.

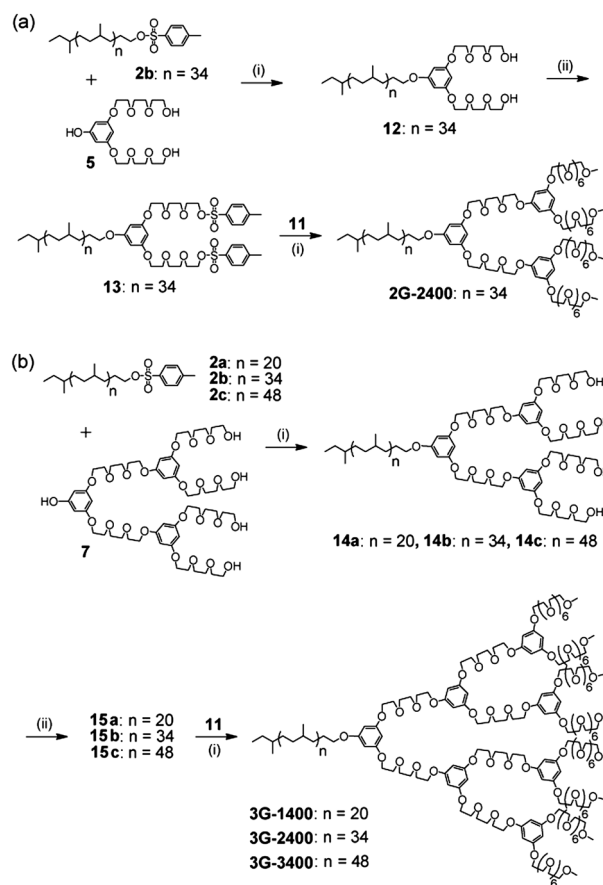
respectively. Due to the different pK_a values, only the phenol group can be deprotonated under potassium carbonate (K_2CO_3) and thereby participate in the Williamson etherification, e.g. the etherification between **4** and **5** in Scheme 1(b). After the chain growth, the focal phenolic group can be regenerated by debenzoylation using Pd/C and H_2 .

Similarly, the peripheral component, i.e. diPEGylated phloroglucinol (**11**), consisting of two poly(ethylene glycol) monomethyl ethers (DP = 7), was prepared by the etherification of monobenzylated phloroglucinol with tosylated PEO coils and subsequent debenzoylation (Scheme 1(c)).

The Williamson etherification and the tosylation of terminal alcohols were identically applied to the divergent synthesis of the final dendron-coils (Scheme 2). The PEP coils with tosyl ends (**2b** and **2c**) were reacted with the excess of dibranched and tetra-branched branching components (**5** and **7**) in the presence of K_2CO_3 , yielding intermediate compounds **12** and **14b–c**. It is because the remaining branching components were easily removed by the selective precipitation of the products in methanol. On the other hand, another intermediate **14a**, with the shortest PEP block, was not precipitated in methanol. Thus, in the coupling reaction with **7**, the excess of **2a** was used for a convenient column chromatography. In the TLC, after the reaction, the leftover of hydrophobic **2a** had a much larger R_f value than **14a**.

Next, the conversion of the terminal alcohols of **12** and **14a–c** into tosyl ends and the subsequent etherification with the excess of the peripheral component (**11**) resulted in the final dendron-coil copolymers. The purification of the final dendron-coils was performed by a combination of silica-column chromatography and preparative gel permeation chromatography (GPC) techniques. After purification, the dendron-coils were characterized by NMR spectroscopies, GPC, and matrix-assisted laser desorption/ionization time-of-flight mass spectrometry (MALDI-TOF MS).

The 1H - and ^{13}C -NMR spectra of the final dendron-coils are shown in Fig. 2. By comparing the integration areas of aromatic (assigned as *c*) and ethylene oxide parts, the numbers of the phloroglucinol protons were calculated to be 9 and 21 for **2G-2400** and the 3rd generation series, respectively. In addition, the integration value of the terminal methoxy protons (assigned as *i*) of **3G-2400** with respect to the identical PEP (assigned as *a* and *b*) is nearly twice as large as **2G-2400** (Fig. 2(a) and (c)). These 1H NMR data strongly suggest that the peripheral components (**11**) were completely coupled with **13** and **14a–c** in the final Williamson reaction, and thus the resulting dendron-coils have no structural defects on the periphery. At the same time, the integration area of the PEP part (assigned as *a* and *b*) relative to the identical aromatic proton area increases proportionally to the PEP molecular weight. The number-average degree of polymerization (DP) of the linear PEP was calculated to be 20, 34, and 48 for **3G-1400**, **3G-2400**, and **3G-3400**, respectively (Fig. 2(b)–(d)). On the basis of these integration analyses, the number average molecular weights (M_n) were calculated, and they quantitatively matched the expected values (Table 2). In addition to the proton NMR results, eleven distinct carbon signals were observed in the ^{13}C NMR spectra of the dendron-coils, which corroborates the successful synthesis as designed (Fig. 2(e)–(h)).



Scheme 2 Divergent synthetic routes of (a) **2G-2400** and (b) 3rd generation series (**3G-1400**, **3G-2400**, and **3G-3400**). Reagents and conditions: (i) K_2CO_3 , KI, CH_3CN and (ii) TsCl, pyridine, CH_2Cl_2 .

All dendron-coils showed narrow molecular weight distributions (M_w/M_n) of less than 1.02 in the GPC data, indicative of high purities (Fig. 3(a) and Table 2). It is interesting to note that **2G-2400** showed a smaller retention volume than **3G-1400**, which is in contrast to the molecular weights calculated from the 1H NMR spectra (Fig. 3(a) and Table 2). This mismatch is

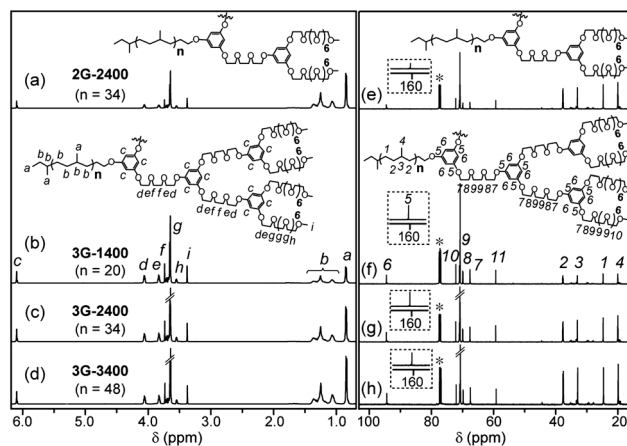


Fig. 2 1H - (left) and ^{13}C - (right) NMR spectra of (a and e) **2G-2400**, (b and f) **3G-1400**, (c and g) **3G-2400**, and (d and h) **3G-3400**.

Table 2 Characterization of dendron-coils

Dendron-coil	$M_n/\text{g mol}^{-1}$		M_w/M_n^c	Hydrophilic volume fraction (f)	Morphology ^d	Lattice parameter/nm	TODT/ $^{\circ}\text{C}$
	NMR ^a	MS ^b					
2G-2400	4300	4320	1.02	0.37	LAM	11.1 ^e	183
3G-1400	5570	5560	1.02	0.69	MC	22.4 ^f	158
3G-2400	6550	6560	1.02	0.57	COL	14.9 ^e	Not shown ^h
3G-3400	7520	7520	1.02	0.48	COL	18.8 ^e	Not shown ^h
					LAM	11.3 ^g	

^a Determined from the $^1\text{H-NMR}$ spectra. ^b Determined from the MALDI-TOF MS data. ^c Determined from the GPC data. ^d LAM: lamellar, MC: micellar cubic, COL: columnar. ^e Determined at $30\text{ }^{\circ}\text{C}$. ^f Determined at $155\text{ }^{\circ}\text{C}$. ^g Determined at $200\text{ }^{\circ}\text{C}$. ^h No TODT was detected up to $200\text{ }^{\circ}\text{C}$.

attributed to the more compact globular shape of highly branched **3G-1400** than **2G-2400** in the THF solution.⁶ Indeed, the accurate molecular weights were determined by the MALDI-TOF MS. Fig. 3(b) shows the narrow and symmetric MALDI-TOF MS spectra, which provide the direct evidence that there are no structural defects. The molecular weights of the highest peak are 4320 g mol^{-1} , 5560 g mol^{-1} , 6560 g mol^{-1} , and 7520 g mol^{-1} for **2G-2400**, **3G-1400**, **3G-2400**, and **3G-3400**, respectively.

To interpret the morphological behavior of the final dendron-coils in the next section, it would be helpful to determine the dendron volume fractions (f). In the f calculations, we assumed that the densities of the hydrophobic PEP and the hydrophilic part (PEO-like dendritic branches plus peripheral PEOs) are 0.79 g cm^{-3} and 1.06 g cm^{-3} , respectively.⁷ The calculated f s were 0.37, 0.69, 0.57, and 0.48 for **2G-2400**, **3G-1400**, **3G-2400** and **3G-3400**, respectively.

Thermal and self-assembling properties

Melting and glass transition temperatures (T_m and T_g) were investigated by differential scanning calorimetry (DSC), scanning from -70 to $50\text{ }^{\circ}\text{C}$ (Fig. 4). Among the polymers, only **2G-2400**, with the smaller 2nd generation dendron, showed a T_m at $-3.1\text{ }^{\circ}\text{C}$. Considering the molecular composition, the T_m corresponds to

the melting of the peripheral PEO chains. The heat of fusion was estimated to be 18.8 J g^{-1} , on the basis of which its crystallinity was calculated to be 38.7%, by comparing the heat of fusion of the perfect crystalline PEO chain.⁸ In contrast, the 3rd generation series with the larger dendron exhibited no PEO melting transition, while the T_g s were observed near $-51\text{ }^{\circ}\text{C}$ in all cases. This might be because the semi-crystalline peripheral PEOs were plasticized by the larger 3rd generation dendritic core, resulting in the complete suppression of PEO crystallization.⁹

The incompatibility between hydrophobic PEP and PEO blocks led to ordered phases (*i.e.*, mesophase) in the melt. As consistent with the polymer design concept in the Introduction, all mesophases could be observed at ambient temperature, and persisted up to temperatures above $150\text{ }^{\circ}\text{C}$. The temperature-variable small angle X-ray scattering (SAXS) and dynamic mechanical spectroscopy (DMS) experiments verified order–order and order–disorder transition temperatures (OOT and TODT), and the structural information in each mesophase. **2G-2400** and **3G-1400** exhibited their TODTs at $183\text{ }^{\circ}\text{C}$ and $158\text{ }^{\circ}\text{C}$, respectively, while **3G-2400** and **3G-3400** maintained their ordered phases up to the experimentally accessible temperature of $240\text{ }^{\circ}\text{C}$.

2G-2400 with $f = 0.37$ formed a mesophase that turned into a disordered liquid at $183\text{ }^{\circ}\text{C}$ (Fig. 5). The SAXS pattern at $30\text{ }^{\circ}\text{C}$ showed four reflections with q -spacing ratios of 1 : 2 : 3 : 4, indicative of a lamellar structure (Fig. 6(a)). It has been known that the elastic modulus (G') representing the overall elasticity of

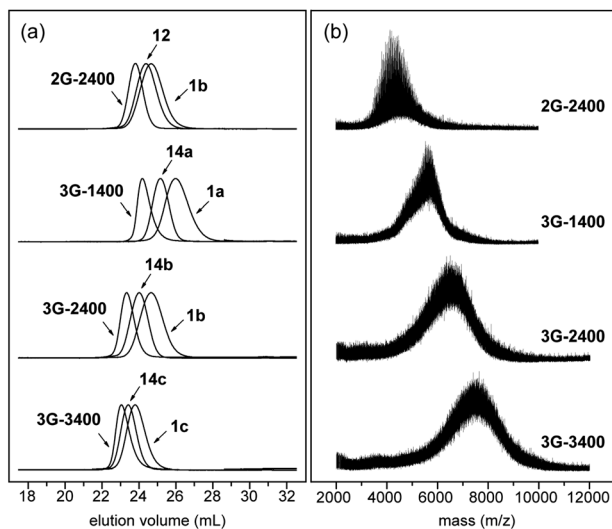


Fig. 3 (a) GPC elugrams and (b) MALDI-TOF MS data of dendron-coils.

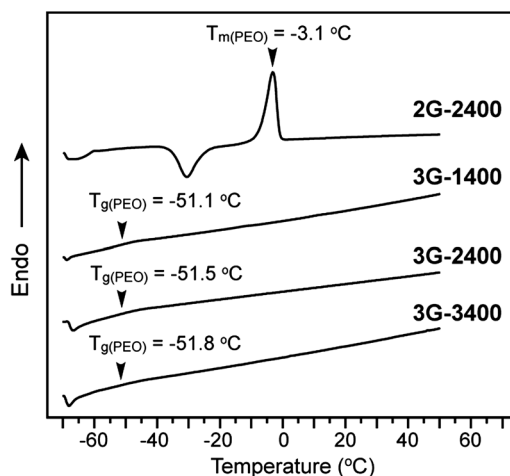


Fig. 4 DSC thermograms of dendron-coils.

a system increases as the structural dimensionality increases.¹⁰ Therefore, the SAXS result is consistent with the DMS data where the mesophase exhibits relatively low G' near 10^4 Pa. Because lamellar morphology is one-dimensionally periodic, the degree of shear-induced deformations in a polydomain lamellar sample is smaller than two-dimensionally periodic cylindrical and three-dimensionally cubic structures.

From the observed primary peak, d -spacing was estimated to be 11.1 nm (Table 2). To understand the packing structure, *e.g.*, bilayered or interdigitated monolayered, in the lamellar mesophase, we calculated the molecular section which was assumed to be a square column. By comparing the height of the molecular section with the d -spacing, we could determine the molecular packing of the lamellar structure. In the calculation, the fully stretched length of the peripheral PEO chain was estimated to be 3.2 nm from the CPK model, and the cross-sectional area of the square column was determined to be 0.71 nm^2 . Then, by dividing the molecular volume by the cross-sectional area, the height of the molecular section was found to be 10.7 nm, which is almost identical to the d -spacing of 11.1 nm from the SAXS data. Therefore, **2G-2400** self-assembles into an interdigitated monolayer, which contrasts the bilayered lamellar structure of linear block copolymers (Fig. 7). The formation of an interdigitated monolayer rather than the bilayered packing is driven by the conformational entropy of the longer PEP coil; otherwise, the bilayered structure would be enthalpically favored because of the minimal interfacial area between the two blocks. As compared to the bilayered lamellar, the cross-section of the PEP coil in the interdigitated packing is twice larger, by which PEP coils reside in a less anisotropic space (Fig. 7). Consequently, the PEP coil is less stretched.

Morphological behavior in the 3rd generation series with the identical dendron can be elucidated as a function of the dendron volume fraction (f). The SAXS spectra of the 3rd generation series are presented in Fig. 6.

3G-1400 with $f = 0.69$ exhibited a mesophase before disordering at $158 \text{ }^\circ\text{C}$ in the DMS data (Fig. 5). In addition, the G' values in this mesophase were above 10^6 Pa, which indicates the high elasticity of the mesophase. This magnitude in G' is typically observed in cubic mesophases, because of the large free energy cost occurring from the deformations of highly symmetric

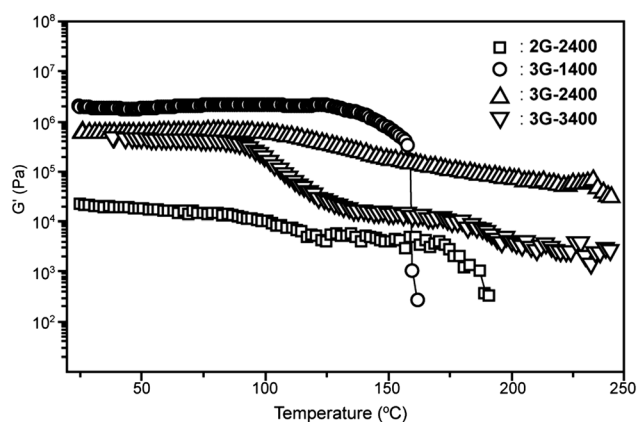


Fig. 5 Dynamic mechanical spectroscopy data of dendron-coils as a function of temperature.

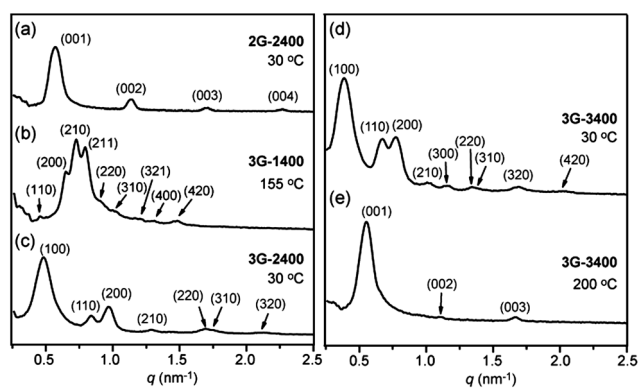


Fig. 6 SAXS data of (a) **2G-2400**, (b) **3G-1400**, (c) **3G-2400**, and (d and e) **3G-3400**.

three-dimensional cubic lattices.^{1e,11} Therefore, the DMS data suggest a cubic mesophase.

The SAXS data of **3G-1400** at $155 \text{ }^\circ\text{C}$ showed a large number of reflections (Fig. 6(b)). These SAXS peaks can be indexed as the (110), (200), (210), (211), (220), (310), (321), (400), and (420) of a $Pm3n$ cubic symmetry (Table 3), which is consistent with the DMS results. From the dimension of the (200) reflection, the cubic lattice parameter was calculated to be 22.4 nm.

As the PEP length increased, **3G-2400** with $f = 0.57$ displayed seven peaks with q -spacing ratios of $1 : \sqrt{3} : \sqrt{4} : \sqrt{7} : \sqrt{12} : \sqrt{13} : \sqrt{19}$ at $30 \text{ }^\circ\text{C}$ (Fig. 6(c)). The reflections can be assigned as the (100), (110), (200), (210), (220), (310), and (320) planes of a 2-D hexagonal columnar structure (Table 3). The observed multiple reflections are not common in typical hexagonal columnar mesophases, which usually show three or four reflections at most. The SAXS results indicate that microphase-separated cylinders well-organize into a 2-D hexagonal lattice, which might be due to the great immiscibility between the hydrophilic PEO-like dendrons and the hydrophobic PEP coils. From the d -spacing of the (100) plane, the inter-columnar distance (a) was calculated to be 14.9 nm.

As the PEP length further increased, **3G-3400** with $f = 0.48$ displayed two different mesophases as a function of temperature. As shown in the DMS data, the G' began to drop near $90 \text{ }^\circ\text{C}$, after which another plateau region appeared. By considering the



Fig. 7 Interdigitated lamellar model of **2G-2400**.

Table 3 The measured distances ($d_{\text{meas}} = 2\pi/q$) and corresponding (hkl) indexation data of the observed SAXS reflections for the micellar cubic and hexagonal columnar phases. d_{calcd} is the calculated distance based on the lattice parameter of each structure

hkl	$Pm\bar{3}n$ cubic ^a		Hexagonal columnar ^b			
	3G-1400		3G-2400		3G-3400	
	$d_{\text{meas}}/\text{nm}$	$d_{\text{calcd}}/\text{nm}$	$d_{\text{meas}}/\text{nm}$	$d_{\text{calcd}}/\text{nm}$	$d_{\text{meas}}/\text{nm}$	$d_{\text{calcd}}/\text{nm}$
100			12.9	12.9	16.3	16.3
110	13.8	13.8	7.5	7.4	9.4	9.4
200	9.7	9.7	6.5	6.5	8.1	8.2
210	8.6	8.6	4.9	4.9	6.2	6.2
211	7.9	7.9				
300					5.4	5.4
220	7.0	6.9	3.7	3.7	4.7	4.7
310	6.3	6.2	3.6	3.6	4.5	4.5
320			2.9	3.0	3.7	3.7
321	5.3	5.2				
400	4.8	4.9				
420	4.2	4.3			3.1	3.1

^a Data at 155 °C. ^b Data at 30 °C.

magnitude of the elastic modulus in each mesophase, the morphologies in the lower and higher temperatures can be suggested to be hexagonal columnar and lamellar structures, respectively. Indeed, the SAXS data exhibited the expected 2-D hexagonal columnar and lamellar reflection patterns (Fig. 6(d)). The columnar phase of **3G-3400** displayed an even larger number of well-resolved reflections than that of **3G-2400** (Table 3). The inter-columnar distance (a) of the columnar mesophase at 30 °C was 18.8 nm, and the periodic layer thickness of the lamellar mesophase at 200 °C was 11.3 nm. By a similar lamellar packing consideration to **2G-2400**, the height of the molecular section was calculated to be 9.2 nm. Thus, the observed periodic dimension suggests an interdigitated monolayer.

At the identical 3rd generation dendron, the increase of the PEP coil length (*i.e.* the decrease of f) must lead to continuous PEP domains. Therefore, the cubic morphology of **3G-1400** strongly suggests a micellar cubic structure because **3G-2400** and **3G-3400** with longer PEP coils exhibited columnar structures. The phase sequence of micellar to columnar structures with decreasing f is the most plausible option. The micellar cubic phase with $Pm\bar{3}n$ symmetry is referred to as A15 phase consisting of eight micelles in a unit cell (Fig. 8). This micellar cubic structure was frequently found in dendritic molecules, but it has not been observed in

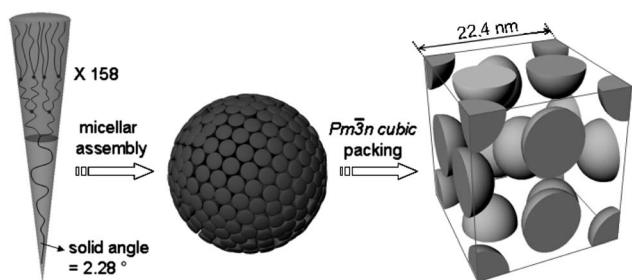


Fig. 8 Formation of the micellar cubic mesophase with $Pm\bar{3}n$ symmetry of **3G-3400**. For clarity, the hydrophilic matrix is omitted in the picture on the right.

linear block copolymers which display a body-centered micellar cubic structure.^{9,12} In the proposed structure, the micellar core is comprised of hydrophobic PEPs, while hydrophilic dendrons constitute the outer matrix. On the basis of the SAXS data and the molecular volume, the number (N_m) of molecules occupying a single micelle and the solid angle of the cone-shape molecule was calculated to be approximately 158 and 2.28°, respectively.^{1a,13}

On the basis of the SAXS data, 4.6 Å thick column stratum and relevant densities, the numbers of molecules per column cross-section could be obtained using the following equation: $N_c = 4.6 \text{ \AA} \times a \times d_{(100)}/V_m$, where a and V_m are the lattice parameter and molecular volume, respectively.¹⁴ The numbers were calculated to be 7.7 and 10.4 for **3G-2400** and **3G-3400**, respectively. The increase in N_c can be explained by a molecular wedge angle (α) depending on the PEP coil length. From the N_c , the angles were calculated to be 46.8° and 34.6° for **3G-2400** and **3G-3400**, respectively. For the identical 3rd generation dendron, the increase of the PEP coil length decreases the molecular wedge angle in the columnar structure (Fig. 9).

Considering the observed morphological results as a function of f , the introduction of the dendritic block shifts the phase boundaries toward smaller dendron volume fractions (*i.e.* larger volume fractions of linear PEP) when compared to conventional linear block copolymers.¹⁵ The above phase boundary argument is even manifested in the 3rd generation series, as the asymmetric factor becomes greater due to the larger 3rd generation dendron.

Our dendron-coil system is also different from block copolymers bearing rigid π -conjugated dendrons. Since our polyether dendrons are conformationally flexible, the dendron conformation can be tuned depending on the PEP coil length, resulting in the various morphologies. In contrast, shape-persisted dendrons preferentially lead to 2-D columnar structures with inherent curvature. Indeed, a dendron-coil system based on dendritic poly(phenylazomethine)s exclusively showed 2-D columnar structures over a wide range of dendron volume fractions, 0.38 < f < 59.¹⁶

It should be noted that the temperature-dependent transformation in **3G-3400** is the complete reversal of the phase sequence (*i.e.* from lamellar to gyroid, columnar, and micellar

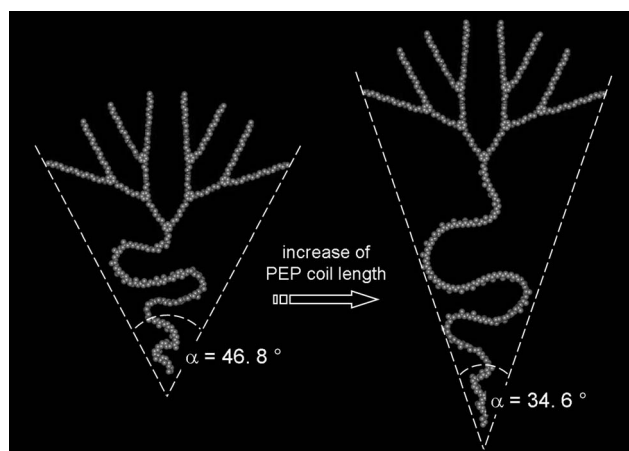


Fig. 9 Molecular wedges of **3G-2400** and **3G-3400** in the columnar structure.

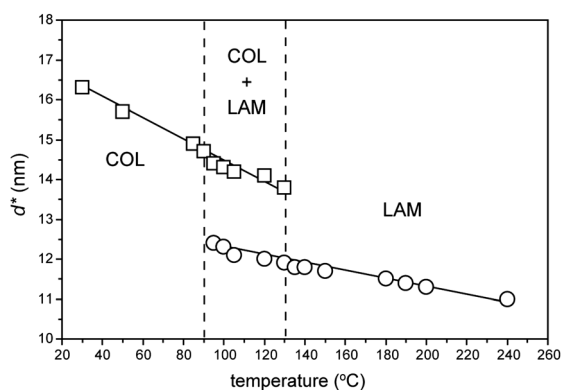


Fig. 10 Principal d -spacing (d^*) of **3G-3400** as a function of temperature.

upon heating) in linear block copolymers.¹⁷ This remarkable contrast can be explained in terms of chain topologies. For the columnar morphology of linear block copolymers, a longer coil occupies the outer matrix, while a shorter block is located in the inner core. In this arrangement, the longer coil adopts more stable conformations at the expense of the conformational energy of the shorter coil, which reduces the overall free energy. In contrast, for the columnar structure of the dendron-coil system in this study, the dendron block tends to be located in the outer matrix, while the longer PEP coil is in the inner core (Fig. 9). By considering the above-mentioned wedge angles, the longer PEP coil of **3G-3400** can be thought to be more stretched than the PEP coil of **3G-2400**. This must be the reason for the thermally induced transition from columnar to lamellar structures in **3G-3400**. As the temperature increases, however, the conformational energy of the stretched PEP coil in the columnar phase becomes destabilized. In the end, the columnar morphology has to be converted into the interdigitated lamellar structure, which allows the PEP coil to be less stretched. This argument can be confirmed by a plot of the principal d -spacing (d^*) as a function of temperature. The d^* are the $d_{(100)}$ and $d_{(001)}$ spacings for the columnar and lamellar structures, respectively. As shown in Fig. 10, a sudden reduction in d^* can be observed. This spacing decrease at the transition indicates that highly stretched PEP conformations change into less-stretched ones.

Conclusions

We prepared a series of dendron-coil block copolymers without any structural defect by way of a divergent method. The dendritic and linear blocks are hydrophilic polyether dendrons with 2nd and 3rd generations and hydrophobic PEP coils with different coil lengths, respectively. **2G-2400** with a 2nd generation exhibited a PEO melting transition, while no PEO melting transition was shown in the 3rd generation series, *i.e.* **3G-1400**, **3G-2400**, and **3G-3400**. Depending on the dendron generation and the dendron volume fraction (f), diverse microphase-separated morphologies were revealed due to the strong segregation tendency between the PEO-like dendron and PEP blocks. The 2nd generation dendron-coil, **2G-2400** with $f = 0.37$, self-assembled into a lamellar structure with an interdigitated dendron packing. For the 3rd generation series, A15 micellar cubic, hexagonal columnar, and lamellar morphologies were shown as the PEP coil length and/or

temperature increased. An unusual phase transition from columnar to lamellar structures was observed in **3G-3400**. This temperature dependent phase transition is the complete reversal of the phase sequence of linear block copolymers. Remarkably, in the observed micellar and columnar morphologies in this study, the continuous matrix consists of hydrophilic dendrons, which can be an excellent structural platform for the next-generation electrolyte materials.

Experimental

General methods

¹H- and ¹³C-NMR spectra were recorded at room temperature on Varian 200 and Varian 500 spectrometers, using chloroform-*d* (CDCl₃) as the solvent and tetramethylsilane (TMS) as the internal reference for chemical shifts. The final products were purified with a LC-9201 recycling preparative HPLC (Japan Analytical Industry) equipped with a PI-50 pump, a UV detector/310, a RI detector/RI-50s, and three JAIGEL-1H, 2H, 2.5H columns (600 × 20 mm²). Chloroform was used as the eluent at a flow rate of 3.5 mL min⁻¹. The purity of the products was checked by thin-layer chromatography (TLC; Merck, silica gel 60). Gel permeation chromatography (GPC) measurements were conducted in THF and *N,N'*-dimethylacetamide (99.9%) (98 : 2 volume ratio) using a Waters 401 instrument equipped with KF-802, KF-803, AT-G and AT-804S Shodex columns at a flow rate of 1.0 mL min⁻¹. Monodisperse linear polystyrene standards were used for calibration. THF (with 2% v/v *N,N'*-dimethylacetamide) was used as the eluent, and the rate was 1.0 mL min⁻¹ at 35 °C. Matrix-assisted laser desorption/ionization time-of-flight (MALDI-TOF) mass spectra were obtained on a Perceptive Biosystems Voyager-DE STR system equipped with a 337 nm nitrogen laser, using dithranol as the matrix. Mass spectra were acquired in reflector mode at an acceleration voltage of +20 kV. A Perkin Elmer DSC-7 was used to determine thermal transitions. In all cases, heating and cooling scans were measured at a rate of 10 °C min⁻¹. X-Ray scattering measurements were performed in transmission mode with synchrotron radiation at the 10C1 beam line of the Pohang Accelerator Laboratory (PAL), Korea. The sample was held in an aluminium sample holder with films on both sides. All dynamic mechanical spectroscopy (DMS) data were recorded on a Rheometrics Solid Analyzer RSA 2 equipped with a shear sandwich geometry (0.5 mm thickness). Dynamic mechanical spectrometer was operated at small strain (1%) and low frequency (1 rad s⁻¹), and temperature ramps were conducted at 2 °C min⁻¹. Dynamic elastic (G') moduli were recorded as a function of temperature.

Synthesis

The general synthetic procedures are outlined in Schemes 1 and 2.

Compounds 2a–c. Hydroxyl-terminated poly(ethylene-*alt*-propylene)s, **PEP-OHs (1a–c)**, with three different number-average molecular weights were synthesized according to a literature method.¹⁸ Compounds **2a–c** were synthesized using the same procedure. A representative synthesis is described for compound **2a**. **1a** ($M_n = 1430$ g mol⁻¹, 8.0 g, 5.6 mmol, 1.0 equiv.), 4-toluenesulfonyl chloride (5.34 g, 28 mmol, 5.0 equiv.)

and pyridine (2.21 g, 28 mmol, 5.0 equiv.) were dissolved in 60 mL of anhydrous CH_2Cl_2 . The reaction mixture was stirred for 24 h at room temperature. The resulting mixture was treated with 1 M HCl solution, and washed with brine. After removal of the solvent under reduced pressure, the residue was purified thrice by dissolution/precipitation with CH_2Cl_2 /methanol to yield a colourless viscous oil (7.9 g, 90%). ^1H NMR (CDCl_3 , δ , ppm): 0.85 (m, 60H, CH_3), 0.97–1.45 (br, 140H, CH and CH_2), 2.45 (s, 3H), 4.04 (t, 2H), 7.34 (d, 2H), 7.79 (d, 2H). M_w/M_n (GPC) = 1.08.

Compound 2b. Yield: 86%. ^1H NMR (CDCl_3 , δ , ppm): 0.85 (m, 102H, CH_3), 0.97–1.45 (br, 238H, CH and CH_2), 4.04 (t, 2H), 2.45 (s, 3H), 7.34 (d, 2H), 7.79 (d, 2H). M_w/M_n (GPC) = 1.05.

Compound 2c. Yield: 91%. ^1H NMR (CDCl_3 , δ , ppm): 0.85 (m, 144H, CH_3), 0.97–1.45 (br, 336H, CH and CH_2), 2.45 (s, 3H), 4.04 (t, 2H), 7.34 (d, 2H), 7.79 (d, 2H). M_w/M_n (GPC) = 1.03.

Compound 4. Compound 3 (ref. 19) (4.5 g, 9.37 mmol), 4-toluenesulfonyl chloride (9.0 g, 47 mmol) and pyridine (3.7 g, 47 mmol) were dissolved in 60 mL of anhydrous CH_2Cl_2 at room temperature. The reaction mixture was stirred for 3 days. After removal of the solvent under reduced pressure, the resulting mixture was dissolved with CH_2Cl_2 and treated with diluted HCl. Then, the solution was washed with brine and concentrated under reduced pressure. The residue was purified by silica column chromatography (CH_2Cl_2 : ethyl acetate = 9 : 1) to yield a brownish oil (5.8 g, 78%). ^1H NMR (CDCl_3 , δ , ppm): 7.78 (d, J = 8.2 Hz, 4H), 7.32 (m, 5H), 7.31 (d, J = 8.2 Hz, 4H), 6.16 (d, J = 1.6 Hz, 2H), 6.11 (d, J = 1.6 Hz, 1H), 4.99 (s, 2H), 4.15 (m, 4H), 4.05 (m, 4H), 3.78 (m, 4H), 3.69 (m, 12H), 2.42 (s, 6H). ^{13}C -NMR (CDCl_3 , δ , ppm): 160.5, 144.8, 136.8, 133.0, 129.9, 128.6, 128.0, 127.6, 94.6, 94.4, 70.9, 70.1, 69.8, 69.4, 68.8, 67.5, 21.8.

Compound 5. To a solution of compound 3 (9.6 g, 20 mmol) in anhydrous CH_3OH (45 mL) was added 10% Pd/C (20 wt%, 1.92 g), and the reaction solution was degassed for 5 times with hydrogen. Then, the reaction mixture was stirred at room temperature for 24 hours in the presence of H_2 . Then, the Pd catalyst was filtered off and the filtrate was concentrated under reduced pressure. The residue was purified by silica column chromatography (ethyl acetate : CH_3OH = 19 : 1 to 8 : 1) to yield a colourless oil (6.5 g, 83%). ^1H NMR (CDCl_3 , δ , ppm): 6.07 (s, 2H), 6.04 (s, 1H), 4.05 (m, 4H), 3.80 (m, 4H), 3.69 (br, 12H), 3.60 (m, 4H), 3.10 (br, 1H), 1.99 (br, 1H). ^{13}C -NMR (CDCl_3 , δ , ppm): 160.5, 158.0, 95.6, 94.3, 72.5, 70.8, 70.4, 69.8, 67.5, 61.8.

Compound 6. To a solution of 4 (2.9 g, 3.67 mmol) and 5 (3.2 g, 8.2 mmol) in anhydrous acetonitrile (40 mL) were added K_2CO_3 (1.78 g, 12.8 mmol) and KI (0.61 g, 3.67 mmol), and the reaction mixture was stirred at 95 °C for 30 hours under nitrogen. The resulting solution was cooled to room temperature and concentrated under reduced pressure. The resulting mixture was dissolved with CH_2Cl_2 , carefully treated with diluted HCl, washed with brine, and concentrated under reduced pressure. The residue was purified by silica column chromatography (ethyl acetate : CH_3OH = 9 : 1 to 3 : 2) to yield a yellowish viscous liquid (3.7 g, 82%). ^1H NMR (500 MHz, CDCl_3 , δ , ppm): 7.36

(m, 5H), 6.17 (d, J = 2.0 Hz, 2H), 6.11 (m, 7H), 4.97 (s, 2H), 4.05 (m, 16H), 3.81 (m, 16H), 3.68 (m, 32H), 3.58 (m, 8H), 2.96 (br, 4H). ^{13}C -NMR (125 MHz, CDCl_3 , δ , ppm): 160.4, 136.8, 128.5, 127.9, 127.5, 94.4, 72.5, 70.7, 70.3, 69.9, 69.6, 67.3, 61.6. Anal. calcd for $\text{C}_{61}\text{H}_{92}\text{O}_{25}$: C, 59.79; H, 7.57%, found: C, 59.73; H, 7.53%.

Compound 7. To a solution of compound 6 (3.1 g, 20 mmol) in anhydrous CH_3OH (35 mL) was added 10% Pd/C (40 wt%, 1.24 g). The reaction solution was degassed 5 times with hydrogen gas and was stirred at room temperature for 24 hours in the presence of H_2 . Then, the Pd catalyst was filtered off and the filtrate was concentrated under reduced pressure. The residue was purified by silica column chromatography (CH_2Cl_2 : CH_3OH = 97 : 3 to 93 : 7) to yield a colourless oil (2.3 g, 79%). ^1H NMR (CDCl_3 , δ , ppm): 6.09 (s, 7H), 6.03 (s, 2H), 4.05 (m, 16H), 3.80 (m, 16H), 3.69 (br, 32H), 3.60 (m, 8H), 2.89 (br, 4H). ^{13}C NMR (CDCl_3 , δ , ppm): 160.5, 160.4, 158.2, 95.3, 94.6, 93.8, 72.6, 70.8, 70.4, 69.8, 67.4, 61.8.

Compound 9. To a solution of poly(ethylene glycol) monomethyl ether (M_n = 350 g mol $^{-1}$, 30 g, 85.7 mmol, 1.0 equiv.) and 4-toluenesulfonyl chloride (49 g, 258 mmol, 3.0 equiv.) in anhydrous CH_2Cl_2 (100 mL) was added pyridine (20.8 mL, 258 mmol, 3.0 equiv.), and the reaction mixture was stirred for 18 h at room temperature. The resulting mixture was treated with diluted aqueous HCl solution and washed with brine. After removal of the solvent under reduced pressure, the residue was purified by silica-column chromatography (CH_2Cl_2 to CH_2Cl_2 : CH_3OH = 8 : 1) to yield a colourless viscous oil (39 g, 90%). ^1H NMR (CDCl_3 , δ , ppm): 2.43 (s, 3H), 3.36 (s, 3H), 3.4–3.8 (m, 26H), 4.14 (t, 2H), 7.32 (d, 2H), 7.78 (d, 2H). ^{13}C NMR (CDCl_3 , δ , ppm): δ 21.7, 59.0, 68.7, 69.3, 70.6, 71.9, 127.9, 129.8, 132.9, 144.7.

Compound 10. To a solution of 5-benzyloxy resorcinol (8) (2.3 g, 10.65 mmol, 1.0 equiv.) and tosylated PEO (9) (12.33 g, 24.5 mmol, 2.3 equiv.) in anhydrous acetonitrile (100 mL) were added K_2CO_3 (4.41 g, 31.9 mmol, 3.0 equiv.) and KI (1.77 g, 10.64 mmol, 1.0 equiv.). The reaction mixture was stirred for 24 h at 95 °C under nitrogen. The resulting solution was cooled to room temperature and concentrated under reduced pressure. The resulting mixture was re-dissolved in CH_2Cl_2 and carefully treated with diluted aqueous HCl solution. The organic layer was then washed with brine and concentrated under reduced pressure. The residue was purified by silica-column chromatography (EtOAc : CH_3OH = 3 : 2) to yield a colourless viscous oil (5.8 g, 62%). ^1H NMR (CDCl_3 , δ , ppm): 3.35 (s, 6H), 3.52 (t, 4H), 3.55–3.75 (m, 44H), 3.79 (t, 4H), 4.03 (t, 4H), 4.97 (s, 2H), 6.09 (s, 1H), 6.15 (s, 2H), 7.27–7.41 (m, 5H). ^{13}C NMR (CDCl_3 , δ , ppm): 59.1, 67.4, 69.7, 70.1, 70.6, 71.9, 94.4, 94.5, 127.5, 127.9, 128.5, 136.8, 160.5.

Synthesis of 11. To a solution of compound 10 (10.5 g, 11.93 mmol) in anhydrous CH_3OH (50 mL) and CHCl_3 (50 mL) was added 10% Pd/C (20 wt%, 2.1 g). The reaction solution was deoxygenated by five vacuum-refill cycles with hydrogen gas. The reaction mixture was stirred for 38 h at room temperature in the presence of H_2 (30 psi). Then, the Pd catalyst was filtered off and

the filtrate was concentrated under reduced pressure. The residue was purified by silica-column chromatography (CH_2Cl_2 to CH_2Cl_2 : $\text{CH}_3\text{OH} = 19 : 1$) to yield a colourless viscous oil (8.0 g, 85%). ^1H NMR (CDCl_3 , δ , ppm): 3.35 (s, 6H), 3.52 (t, 4H), 3.55–3.75 (m, 44H), 3.79 (t, 4H), 4.03 (t, 4H), 5.99 (s, 1H), 6.05 (s, 2H), 7.53 (br, 1H). ^{13}C NMR (CDCl_3 , δ , ppm): 59.1, 67.4, 69.7, 70.6, 71.9, 93.7, 95.4, 158.4, 160.5.

Compounds 12 and 14a–c. Compounds **12** and **14a–c** were synthesized using the similar procedure except for the stoichiometry of reactants and purification. A representative synthesis is described for compound **14a**. To a solution of compound **2a** (1.97 g, 1.24 mmol, 2.0 equiv.), **7** (0.7 g, 0.62 mmol, 1.0 equiv.) in anhydrous acetonitrile (7 mL) and THF (21 mL) were added K_2CO_3 (256 mg, 1.85 mmol, 3.0 equiv.) and KI (205 mg, 1.23 mmol, 2.0 equiv.). The reaction mixture was stirred for 48 h at 95 °C under nitrogen. The resulting solution was cooled to room temperature and concentrated under reduced pressure. The resulting mixture was dissolved with CH_2Cl_2 , carefully treated with diluted aqueous HCl solution, and washed with brine. After removal of the solvent under reduced pressure, the residue was purified by silica-column chromatography (CH_2Cl_2 : $\text{CH}_3\text{OH} = 19 : 1$) to yield a colourless viscous oil (1.42 g, 89%). ^1H NMR (CDCl_3 , δ , ppm): 0.85 (m, CH_3), 0.97–1.45 (br, CH and CH_2), 2.58 (t, 4H), 3.61 (m, 8H), 3.71 (m, 32H), 3.84 (m, 16H), 3.89 (t, 2H), 4.07 (m, 16H), 6.08 (s, 4H), 6.11 (s, 5H). ^{13}C NMR (CDCl_3 , δ , ppm): 19.9, 24.7, 32.9, 33.3, 37.6, 61.9, 67.5, 69.8, 70.5, 70.9, 72.7, 94.6, 160.6. M_w/M_n (GPC) = 1.03.

Compound 12. *Reaction conditions:* compound **2b** (5.4 g, 2.16 mmol, 1.0 equiv.), compound **5** (2.53 g, 6.48 mmol, 3.0 equiv.), K_2CO_3 (1.35 g, 9.72 mmol, 4.5 equiv.), KI (360 mg, 2.16 mmol, 1.0 equiv.) in anhydrous acetonitrile (30 mL) and THF (60 mL) at 95 °C for 48 h. Purification: a repetitive dissolution/precipitation method with CH_2Cl_2 /methanol. Yield: 96%. ^1H NMR (CDCl_3 , δ , ppm): 0.85 (m, 102H, CH_3), 0.97–1.45 (br, 238H, CH and CH_2), 2.58 (t, 2H), 3.61 (m, 4H), 3.71 (m, 12H), 3.84 (m, 4H), 3.89 (t, 2H), 4.07 (m, 4H), 6.09 (s, 2H), 6.13 (s, 1H). ^{13}C NMR (CDCl_3 , δ , ppm): 19.9, 24.7, 33.0, 37.6, 61.9, 67.5, 69.8, 70.6, 71.0, 72.6, 113.1, 113.2, 160.5. M_w/M_n (GPC) = 1.03.

Compound 14b. *Reaction conditions:* compound **2b** (1.91 g, 0.75 mmol, 1.0 equiv.), compound **7** (1.27 g, 1.12 mmol, 1.5 equiv.), K_2CO_3 (467 mg, 3.38 mmol, 4.5 equiv.), KI (104 mg, 0.75 mmol, 1.0 equiv.) in anhydrous acetonitrile (7 mL) and THF (28 mL) at 95 °C for 48 h. Purification: a repetitive dissolution/precipitation method with CH_2Cl_2 /methanol. Yield: 92%. ^1H NMR (CDCl_3 , δ , ppm): 0.85 (m, 102H, CH_3), 0.97–1.45 (br, 238H, CH and CH_2), 2.58 (t, 4H), 3.61 (m, 8H), 3.71 (m, 32H), 3.84 (m, 16H), 3.89 (t, 2H), 4.07 (m, 16H), 6.08 (s, 4H), 6.11 (s, 5H). ^{13}C NMR (CDCl_3 , δ , ppm): 20.0, 24.7, 33.0, 33.3, 37.6, 61.9, 67.5, 69.8, 70.6, 71.0, 72.7, 94.6, 160.5. M_w/M_n (GPC) = 1.02.

Compound 14c. *Reaction conditions:* compound **2c** (1.89 g, 0.54 mmol, 1.0 equiv.), compound **7** (0.76 g, 0.67 mmol, 1.24 equiv.), K_2CO_3 (277 mg, 2.0 mmol, 3.9 equiv.), KI (91 mg, 0.54 mmol, 1.0 equiv.) in anhydrous acetonitrile (7 mL) and THF (35 mL) at 95 °C for 48 h. Purification: a repetitive dissolution/precipitation method with CH_2Cl_2 /methanol. Yield: 74%. ^1H NMR (CDCl_3 , δ ,

ppm): 0.85 (m, 144H, CH_3), 0.97–1.45 (br, 336H, CH and CH_2), 2.58 (t, 4H), 3.61 (m, 8H), 3.71 (m, 32H), 3.84 (m, 16H), 3.89 (t, 2H), 4.07 (m, 16H), 6.08 (s, 4H), 6.11 (s, 5H). ^{13}C NMR (CDCl_3 , δ , ppm): 19.9, 24.6, 33.0, 33.3, 37.7, 61.9, 67.5, 69.8, 70.6, 71.0, 72.7, 94.6, 160.5. M_w/M_n (GPC) = 1.02.

Compounds 13 and 15a–c. Compounds **13** and **15a–c** were synthesized using the same procedure. A representative synthesis is described for compound **15a**. To a solution of **14a** (1.34 g, 0.52 mmol, 1.0 equiv.) and 4-toluenesulfonyl chloride (1.97 g, 10.4 mmol, 20 equiv.) in anhydrous CH_2Cl_2 (60 mL) was added pyridine (0.84 mL, 10.4 mmol, 20 equiv.). The reaction mixture was stirred for 24 h at room temperature. The resulting mixture was treated with diluted aqueous HCl solution and washed with brine. After removal of the solvent under reduced pressure, the residue was purified by flash silica-column chromatography (CH_2Cl_2 : $\text{EtOAc} = 9 : 1$ to $7 : 3$) to yield a yellowish viscous solid (1.34 g, 81%). M_w/M_n (GPC) = 1.03. ^1H NMR (CDCl_3 , δ , ppm): 0.85 (m, CH_3), 0.97–1.45 (br, CH and CH_2), 2.42 (s, 12H), 3.56–3.98 (m, 48H), 4.03 (m, 16H), 4.15 (t, 8H), 6.08 (s, 4H), 6.11 (s, 5H), 7.32 (d, 8H), 7.78 (d, 8H).

Compound 13. Yield: 92%. ^1H NMR (CDCl_3 , δ , ppm): 0.85 (m, 102H, CH_3), 0.97–1.45 (br, 238H, CH and CH_2), 2.42 (s, 6H), 3.56–3.98 (m, 12H), 4.03 (m, 4H), 4.15 (t, 4H), 6.08 (s, 3H), 7.32 (d, 4H), 7.78 (d, 4H). M_w/M_n (GPC) = 1.03.

Compound 15b. Yield: 55%. ^1H NMR (CDCl_3 , δ , ppm): 0.85 (m, 102H, CH_3), 0.97–1.45 (br, 238H, CH and CH_2), 2.42 (s, 12H), 3.56–3.98 (m, 48H), 4.03 (m, 16H), 4.15 (t, 8H), 6.08 (s, 4H), 6.09 (s, 5H), 7.32 (d, 8H), 7.78 (d, 8H). M_w/M_n (GPC) = 1.02.

Compound 15c. Yield: 66%. ^1H NMR (CDCl_3 , δ , ppm): 0.85 (m, 102H, CH_3), 0.97–1.45 (br, 238H, CH and CH_2), 2.42 (s, 12H), 3.56–3.98 (m, 48H), 4.03 (m, 16H), 4.15 (t, 8H), 6.08 (s, 4H), 6.09 (s, 5H), 7.32 (d, 8H), 7.78 (d, 8H). M_w/M_n (GPC) = 1.02.

Dendron-coils. Dendron-coils were synthesized using the same procedure. A representative synthesis is described for **3G-1400**. To a solution of **15a** (1.27 g, 0.39 mmol, 1.0 equiv.) and **11** (1.88 g, 2.38 mmol, 6.0 equiv.) in anhydrous acetonitrile (13 mL) and THF (32 mL) were added K_2CO_3 (495 mg, 3.57 mmol, 9.0 equiv.) and KI (132 mg, 0.79 mmol, 2.0 equiv.). The reaction mixture was stirred for 48 h at 95 °C under nitrogen environment. The resulting solution was cooled to room temperature and concentrated under reduced pressure. The resulting mixture was redissolved with CH_2Cl_2 and carefully treated with diluted aqueous HCl solution. The organic layer was washed with brine. After removal of the solvent under reduced pressure, the residue was purified by flash silica-column chromatography (CH_2Cl_2 : $\text{CH}_3\text{OH} = 49 : 1$ to $19 : 1$) and a preparative GPC to yield a yellowish viscous solid (1.47 g, 66%). ^1H NMR (CDCl_3 , δ , ppm): 0.85 (m, 60H, CH_3), 0.97–1.45 (br, 140H, CH and CH_2), 3.37 (s, 24H), 3.53 (t, 16H), 3.60–3.79 (br, 232H), 3.82 (m, 40H), 4.05 (t, 40H), 6.08 (s, 21H). ^{13}C NMR (CDCl_3 , δ , ppm): 19.6, 24.4, 32.7, 37.5, 59.0, 67.3, 69.6, 70.5, 94.2, 160.4. M_w/M_n (GPC) = 1.02.

2G-2400. Yield: 71%. ^1H NMR (CDCl_3 , δ , ppm): 0.85 (m, 102H, CH_3), 0.97–1.45 (br, 238H, CH and CH_2), 3.37 (s, 12H), 3.53 (t, 8H), 3.60–3.79 (br, 112H), 3.82 (m, 16H), 4.05 (t, 16H), 6.08 (s, 9H). ^{13}C NMR (CDCl_3 , δ , ppm): 19.8, 24.5, 32.8, 37.5, 59.0, 67.4, 69.7, 70.7, 71.9, 94.3, 160.5. M_w/M_n (GPC) = 1.02.

3G-2400. Yield: 62%. ^1H NMR (CDCl_3 , δ , ppm): 0.85 (m, 102H, CH_3), 0.97–1.45 (br, 238H, CH and CH_2), 3.37 (s, 24H), 3.53 (t, 16H), 3.60–3.79 (br, 232H), 3.82 (m, 40H), 4.05 (t, 40H), 6.08 (s, 21H). ^{13}C NMR (CDCl_3 , δ , ppm): 19.6, 24.4, 32.7, 37.5, 59.0, 67.3, 69.6, 70.5, 94.2, 160.4. M_w/M_n (GPC) = 1.02.

3G-3400. Yield: 74%. ^1H NMR (CDCl_3 , δ , ppm): 0.85 (m, 144H, CH_3), 0.97–1.45 (br, 336H, CH and CH_2), 3.37 (s, 24H), 3.53 (t, 16H), 3.60–3.79 (br, 232H), 3.82 (m, 40H), 4.05 (t, 40H), 6.08 (s, 21H). ^{13}C NMR (CDCl_3 , δ , ppm): 19.7, 24.4, 32.7, 37.5, 59.0, 67.3, 69.6, 70.6, 94.2, 160.4. M_w/M_n (GPC) = 1.02.

Acknowledgements

This work was supported by the Core Research Program (2009-0084501) through the National Research Foundation (NRF) funded by the Ministry of Education, Science and Technology (MEST), Republic of Korea. We acknowledge the Pohang Accelerator Laboratory (Beamline 10C1), Korea. We thank Prof. Jin Kon Kim at Pohang University of Science and Technology (POSTECH) for dynamic mechanical spectroscopy measurements.

Notes and references

- (a) B. Rosen, C. J. Wilson, D. A. Wilson, M. Peterca, M. R. Imam and V. Percec, *Chem. Rev.*, 2009, **109**, 6275–6540; (b) E. R. Gillies, T. B. Jonsson and J. M. J. Fréchet, *J. Am. Chem. Soc.*, 2004, **126**, 11936–11943; (c) J. C. M. van Hest, D. A. P. Delnoye, M. W. P. L. Baars, M. H. P. Van Genderen and E. W. Meijer, *Science*, 1995, **268**, 1592–1595; (d) J. Iyer, K. Fleming and P. T. Hammond, *Macromolecules*, 1998, **31**, 8757–8765; (e) B.-K. Cho, A. Jain, S. M. Gruner and U. Wiesner, *Science*, 2004, **305**, 1598–1601; (f) X. Duan, F. Yuan, X. Wen, M. Yang, B. He and W. Wang, *Macromol. Chem. Phys.*, 2004, **205**, 1410–1417; (g) S. N. Chvalun, M. A. Shcherbina, A. N. Yakunin, J. Blackwell and V. Percec, *Polym. Sci.*, 2007, **49**, 158–167; (h) K. T. Kim, C. Park, C. Kim, M. A. Winnik and I. Manners, *Chem. Commun.*, 2006, 1372–1374.
- (a) A. W. Bosman, H. M. Janssen and E. W. Meijer, *Chem. Rev.*, 1999, **99**, 1665–1688; (b) K. L. Wooley, C. J. Hawker, J. M. Pochan and J. M. J. Fréchet, *Macromolecules*, 1993, **26**, 1514–1519; (c) J. Song and B.-K. Cho, *Bull. Korean Chem. Soc.*, 2008, **29**, 1167–1172.
- M. A. Hillmyer, F. S. Bates, K. Almdal, K. Mortensen, A. J. Ryan and J. P. A. Fairclough, *Science*, 1996, **271**, 976–978.
- (a) L. Tian and P. T. Hammond, *Macromolecules*, 2006, **18**, 3976–3984; (b) Z. Bo, J. P. Rabe and A. D. Schlüter, *Angew. Chem., Int. Ed.*, 1999, **38**, 2370–2372; (c) H.-Y. Kim, J. Song, S.-H. Kim, E. Lee, J.-K. Lee, W.-C. Zin and B.-K. Cho, *Chem.–Eur. J.*, 2009, **15**, 8683–8686; (d) B.-K. Cho, S.-H. Kim and E. Lee, *J. Polym. Sci., Part A: Polym. Chem.*, 2010, **48**, 2372–2376.
- (a) T. H. Epps, T. S. Bailey, R. Waletzko and F. S. Bates, *Macromolecules*, 2003, **36**, 2873–2881; (b) G. Floudas, B. Vazaiou, F. Schipper, R. Ulrich, U. Wiesner, H. Iatrou and N. Hadjichristidis, *Macromolecules*, 2001, **34**, 2947–2957; (c) Y. Chang, Y. C. Kwon, S. C. Lee and C. Kim, *Macromolecules*, 2000, **33**, 4496–4500; (d) B.-K. Cho, A. Jain, S. M. Gruner and U. Wiesner, *Chem. Commun.*, 2005, 2143–2145; (e) J.-W. Choi and B.-K. Cho, *J. Polym. Sci., Part A: Polym. Chem.*, 2011, **49**, 2468–2473.
- (a) C. J. Hawker, E. E. Malmström, C. W. Frank and J. P. Kampf, *J. Am. Chem. Soc.*, 1997, **119**, 9903–9904; (b) J. Song, H.-Y. Kim and B.-K. Cho, *Bull. Korean Chem. Soc.*, 2007, **28**, 1771–1776.
- (a) L. J. Fetters, D. J. Lohse, D. Richter, T. A. Witten and A. Zirkel, *Macromolecules*, 1994, **27**, 4639–4647; (b) L. Sun, Y. Liu, L. Zhu, B. S. Hsiao and C. A. Avila-Orta, *Polymer*, 2004, **45**, 8181–8193.
- E. Lee, B.-I. Lee, S.-H. Kim, J.-K. Lee, W.-C. Zin and B.-K. Cho, *Macromolecules*, 2009, **42**, 4134–4140.
- Y.-W. Chung, J.-K. Lee, W.-C. Zin and B.-K. Cho, *J. Am. Chem. Soc.*, 2008, **130**, 7139–7147.
- (a) R. G. Larson, K. I. Winey, S. S. Patel, H. Watanabe and R. Bruinsma, *Rheol. Acta*, 1993, **30**, 245–253; (b) C. Y. Ryu, M. S. Lee, D. A. Hajduk and T. P. Lodge, *J. Polym. Sci., Part B: Polym. Phys.*, 1997, **35**, 2811–2823; (c) J. Zhao, B. Majumdar, M. F. Schulz, F. S. Bates, K. Almdal, K. Mortensen, D. A. Hajduk and S. M. Gruner, *Macromolecules*, 1996, **29**, 1204–1215; (d) M. B. Kossuth, D. C. Morse and F. S. Bates, *J. Rheol.*, 1999, **43**, 167–196; (e) S. Förster, A. K. Khandpur, J. Zhao, F. S. Bates, I. W. Hamley, A. J. Ryan and W. Bras, *Macromolecules*, 1994, **27**, 6922–6935.
- (a) R. Mezzenga, P. Schurtenberger, A. Burbidge and M. Michel, *Nat. Mater.*, 2005, **4**, 729–740; (b) C. A. Tyler and D. C. Morse, *Macromolecules*, 2003, **36**, 3764–3774.
- (a) V. S. K. Balagurusamy, G. Ungar, V. Percec and G. Johansson, *J. Am. Chem. Soc.*, 1997, **119**, 1539–1555; (b) V. Percec, C.-H. Ahn, G. Ungar, D. J. P. Yearley, M. Möller and S. S. Sheiko, *Nature*, 1998, **391**, 161–164; (c) Y. Sagara and T. Kato, *Angew. Chem., Int. Ed.*, 2008, **47**, 5175–5178; (d) S. Yazaki, Y. Kamikawa, M. Yoshio, A. Hamasaki, T. Mukai, H. Ohno and T. Kato, *Chem. Lett.*, 2008, 538–539; (e) J.-K. Kim, M.-K. Hong, J.-H. Ahn and M. Lee, *Angew. Chem., Int. Ed.*, 2005, **44**, 328–332.
- D. A. Tomalia, *Soft Matter*, 2010, **6**, 456–474.
- (a) J.-W. Choi, M.-H. Ryu, E. Lee and B.-K. Cho, *Chem.–Eur. J.*, 2010, **16**, 9006–9009; (b) J.-W. Choi and B.-K. Cho, *Soft Matter*, 2011, **7**, 4045–4049.
- (a) G. M. Grason, B. A. DiDonna and R. D. Kamien, *Phys. Rev. Lett.*, 2003, **91**, 58304; (b) G. T. Pickett, *Macromolecules*, 2002, **35**, 1896–1904.
- Y. Gao, X. Zhang, M. Yang, X. Zhang, W. Wang, G. Wegner and C. Burger, *Macromolecules*, 2007, **40**, 2606–2612.
- (a) M. W. Matsen and F. S. Bates, *Macromolecules*, 1996, **29**, 7641–7644; (b) I. W. Hamley, V. Castelletto, G. Floudas and F. Schipper, *Macromolecules*, 2002, **35**, 8839–8845.
- (a) S. C. Schmidt and M. A. Hillmyer, *J. Polym. Sci., Part B: Polym. Phys.*, 2002, **40**, 2364–2376; (b) S. Mahajan, B.-K. Cho, J. Allgaier, L. J. Fetters, G. W. Coates and U. Wiesner, *Macromol. Rapid Commun.*, 2004, **25**, 1889–1894.
- J. Song and B.-K. Cho, *Bull. Korean Chem. Soc.*, 2010, **31**, 1835–1836.